[3]Moore, C.J., "The Role of Shear Layer Instability Waves in Jet Exhaust Noise," *Journal of Fluid Mechanics,* Vol. 80, April 1977, pp. 321-367.
[4]Morrison, G.L. and McLaughlin, D.K., "The Instability Process in Low Reynolds Number Supersonic Jets," *AIAA Journal,* Vol. 18, July 1980, pp. 793-800.
[5]Morrison, G.L. and McLaughlin, D.K., "The Noise Generated by Instabilities in Low Reynolds Number Supersonic Jets," *Journal of Sound and Vibration,* Vol. 65, July 1979, pp. 177-191.
[6]Kendall, J.M., "Supersonic Boundary Layer Stability Experiments," *Proceedings of the Boundary Layer Transition Study Group Meeting,* Vol. II, Aerospace Rept. TR-0158 (S3816-63)-1, 1967.
[7]Morrison, G.L., "Flow Instability and Acoustic Measurements on Low Reynolds Number Supersonic Jets," Ph.D. Dissertation, Oklahoma State University, 1977.
[8]Miksad, R.W., "Experiments on the Non-Linear Stages of Free Shear-Layer Transition," *Journal of Fluid Mechanics,* Vol. 56, Dec. 1972, pp. 695-719.
[9]McLaughlin, D.K., Morrison, G.L., and Troutt, T.R., "Reynolds Number Dependence in Supersonic Jet Noise," *AIAA Journal,* Vol. 15, April 1977, pp. 526-532.
[10]Ahuja, K.K., Lepicovsky, J., and Burrin, R.H., "Acoustic and Turbulence Measurements of a Tone Excited Jet With and Without Flight Simulation," AIAA Paper 81-2007, 1981.

Analytical Approximation of Two-Dimensional Separated Turbulent Boundary-Layer Velocity Profiles

T. W. Swafford*
Sverdrup Technology, Inc.
Arnold Air Force Station, Tennessee

Introduction

THE calculation of separated two-dimensional flow using an inverse formulation of the boundary-layer equations[1-6] is attractive because of simplicity and cost reduction compared to solving the Navier-Stokes equations, providing that solution of the boundary-layer equations yields acceptable engineering accuracy. These computation methods can be classed as either integral or differential. Most integral methods require an analytical description of the boundary-layer velocity profile[1,3,6] such that the integral quantities can be evaluated. The purpose of this Note is to present an analytical representation of two-dimensional turbulent boundary-layer velocity profiles that describes attached and separated flow over the entire domain $0 \le y < \infty$. (This analytic representation was reported earlier,[6] but attention here is focused on the details of the development.) The derivation of this expression is presented and examples given to illustrate the quality of agreement with experimental data. Profile correlations resulting from empirical fits of this expression to measured data are also presented. These correlations, along with the velocity profile representation, allow separated turbulent boundary-layer velocity profiles to be generated as a function of shape factor and momentum thickness Reynolds number. Steps to applying the velocity profile expression are summarized in Table 1.

Received July 12, 1982; revision received Oct. 25, 1982.

*Research Engineer, Computational Fluid Dynamics, AEDC Group. Member AIAA.

Analytical Development

The equation proposed to describe reversed flow velocity profiles on smooth, impermeable, adiabatic walls in incompressible flow is an extension of the expression derived by Whitfield,[7] which is a composite function of the form

$$u^+ = u_i^+ + u_o^+ \tag{1}$$

consisting of an inner expression (u_i^+) originally presented in Ref. 8 and an outer expression (u_o^+) derived in Ref. 7. The inner solution as presented in Ref. 7 is given by

$$u_i^+ = (1/0.09)\tan^{-1}(0.09y^+) \tag{2}$$

where

$$u_i^+ = u_i/u_\tau \qquad y^+ = u_\tau y/\nu \qquad u_\tau = (c_f/2)^{1/2} u_e \tag{3}$$

Assumptions made in deriving Eq. (2) for attached flow[8] are also made herein to retain the form of Eq. (2).

The velocity profile slope at the wall, computed from Eq. (2), is positive for attached flow. A negative slope for separated flow can be obtained by simply taking the negative of Eq. (2) and redefining u_τ as $u_\tau = (|c_f|/2)^{1/2} u_e$. Thus, for u^+ to have the correct value of u_e^+ as $y \to \infty$, u_o^+ must behave as

$$u_o^+ \to \left[u_e^+ - \left(-\frac{\pi}{0.18}\right)\right] \tag{4}$$

as $y \to \infty$. In addition, because u_i^+ behaves correctly near the wall, u_o^+ must approach zero as y approaches zero. Therefore the form considered in Ref. 7,

$$u_o^+ = \left[u_e^+ - \left(-\frac{\pi}{0.18}\right)\right] g\left(\frac{y}{\theta}\right) \tag{5}$$

is retained, where $g(y/\theta)$ has the values of $g(0) = 0$ and $g(\infty) = 1$.

In Ref. 7, the form of $g(y/\theta)$ which gave the best overall fit of measured data was determined to be

$$g\left(\frac{y}{\theta}\right) = \tanh^{1/2}\left[a\left(\frac{y}{\theta}\right)^b\right] \tag{6}$$

where a and b are parameters that are functions of c_f, H, and Re_θ (H is the usual boundary-layer shape factor). It should be emphasized that the parameters a and b are different for each velocity profile. This same functional form of $g(y/\theta)$ is retained in the present work. Therefore the proposed analytical representation of two-dimensional incompressible, attached and separated, turbulent boundary-layer velocity profiles becomes

$$u^+ = \frac{s}{0.09}\tan^{-1}(0.09y^+) + \left(u_e^+ - \frac{s\pi}{0.18}\right)\tanh^{1/2}\left[a\left(\frac{y}{\theta}\right)^b\right] \tag{7}$$

where

$$u_e^+ = \left(\frac{2}{|c_f|}\right)^{1/2} \qquad y^+ = \frac{Re_\theta}{u_e^+}\frac{y}{\theta} \qquad \frac{u}{u_e} = \frac{u^+}{u_e^+} \qquad s = \frac{c_f}{|c_f|} \tag{8}$$

Equation (7) can be rearranged to give the velocity ratio u/u_e as a function of physical distance y, local unit Reynolds number, and local skin friction. Therefore, given u/u_e at three points in the boundary layer, a system of three equations [Eq. (7) at each point] and three unknowns (u_e^+, a, and b) is obtained. The velocity measurements of Simpson[9] and Alber

Table 1 Procedure for computing separated or attached turbulent boundary-layer velocity profiles

Step	Requirement	Comment
1	H and Re_θ are inputs	
2	Compute $c_f = \dfrac{0.3e^{-1.33H}}{(\log_{10}Re_\theta)^{1.74+0.31H}} + (1.1\times10^{-4})\left[\tanh\left(4-\dfrac{H}{0.875}\right)-1\right]$	$u_e^+ = \left(\dfrac{2}{\lvert c_f\rvert}\right)^{1/2}$
3	Compute $s = c_f/\lvert c_f\rvert$	
4	Compute $\dfrac{u}{u_e}(2) = \dfrac{1}{1.95}\left[\tanh^{-1}\left(\dfrac{8.5-H}{7.5}\right)-0.364\right]$	$\dfrac{u}{u_e}\left(\dfrac{y}{\theta}\right)$ at $\dfrac{y}{\theta}=2$
5	Compute $\dfrac{u}{u_e}(5) = 0.155 + 0.795\,\mathrm{sech}\,[0.51(H-1.95)]$	$\dfrac{u}{u_e}\left(\dfrac{y}{\theta}\right)$ at $\dfrac{y}{\theta}=5$ $\mathrm{sech}(z) = \dfrac{1}{\cosh(z)} = \dfrac{2}{e^z+e^{-z}}$
6	Compute $g(2) = \left[\dfrac{u}{u_e}(2) - \dfrac{s}{0.09u_e^+}\tan^{-1}\left(\dfrac{0.18Re_\theta}{u_e^+}\right)\right]\Big/\left(1-\dfrac{s\pi}{0.18u_e^+}\right)$	$g\left(\dfrac{y}{\theta}\right)$ at $\dfrac{y}{\theta}=2$
7	Compute $g(5) = \left[\dfrac{u}{u_e}(5) - \dfrac{s}{0.09u_e^+}\tan^{-1}\left(\dfrac{0.45Re_\theta}{u_e^+}\right)\right]\Big/\left(1-\dfrac{s\pi}{0.18u_e^+}\right)$	$g\left(\dfrac{y}{\theta}\right)$ at $\dfrac{y}{\theta}=5$
8	Compute $b = \ell n\left\{\dfrac{\tanh^{-1}[g^2(2)]}{\tanh^{-1}[g^2(5)]}\right\}\Big/\ell n\left(\dfrac{2}{5}\right)$	$\tanh^{-1}(z) = \tfrac{1}{2}\ell n\left(\dfrac{1+z}{1-z}\right)$
9	Compute $a = \tanh^{-1}[g^2(2)]/2^b$	$\tanh(z) = (e^{2z}-1)/(e^{2z}+1)$
10	$u^+ = \dfrac{s}{0.09}\tan^{-1}(0.09y^+) + \left(u_e^+ - \dfrac{s\pi}{0.18}\right)\tanh^{1/2}\left[a\left(\dfrac{y}{\theta}\right)^b\right]$	$\dfrac{u}{u_e} = \dfrac{u^+}{u_e^+}$ $\quad y^+ = \dfrac{Re_\theta}{u_e^+}\dfrac{y}{\theta}$

et al.[10] were fit using this procedure and the results are presented in Fig. 1. Reasonably good agreement is obtained over the entire range of y for both attached and separated profiles. For separated profiles, a negative skin friction was inferred by knowing, a priori, that the measured velocity near the wall was negative, resulting in $s=-1$. The measurements of Alber et al.[10] were fit by transforming the measured (compressible) variables into equivalent incompressible values.[11]

The usefulness of Eq. (7) appears limited because of its dependence upon u_e^+ (i.e., skin friction) and the parameters a and b. However, by using values of c_f inferred from profile fits of Eq. (7) and Coles' Law of the Wall-Law of the Wake,[12] in addition to those measured directly, an empirical correlation can be established for estimating c_f for both attached and separated flows, analogous to those proposed, e.g., by Ludweig and Tillmann[13] and White,[14] for attached flows.

Figure 2 illustrates these results with c_f plotted as a function of H. The expression chosen to represent these data (shown as a solid line in Fig. 2) is

$$c_f = \frac{0.3e^{-1.33H}}{(\log_{10}Re_\theta)^{1.74+0.31H}} + (1.1\times10^{-4})\left[\tanh\left(4-\frac{H}{0.875}\right)-1\right] \tag{9}$$

The parameters a and b which appear in Eq. (7) are determined by matching the velocity distribution at $y/\theta=2$ and 5 (Ref. 7). The velocity ratios at $y/\theta=2$ and 5 are correlated with H for numerous measured attached and separated velocity profiles and are presented in Fig. 3. The

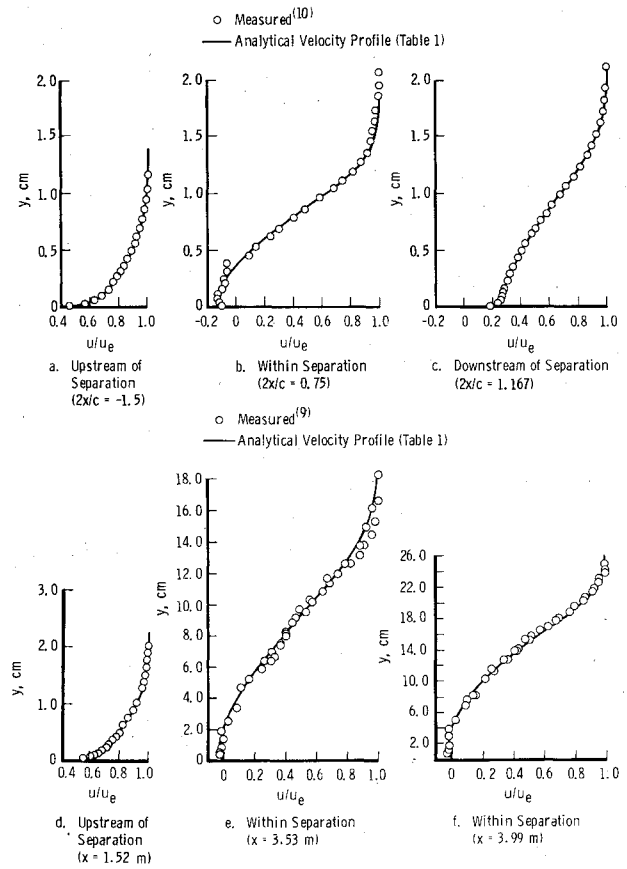

Fig. 1 Comparison of measured attached and separated boundary-layer profiles with the velocity profile in Table 1.

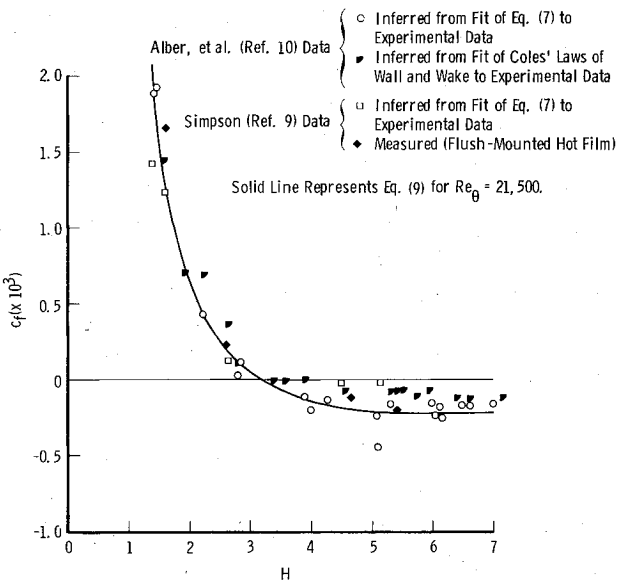

Fig. 2 Correlation of c_f for attached and separated flow.

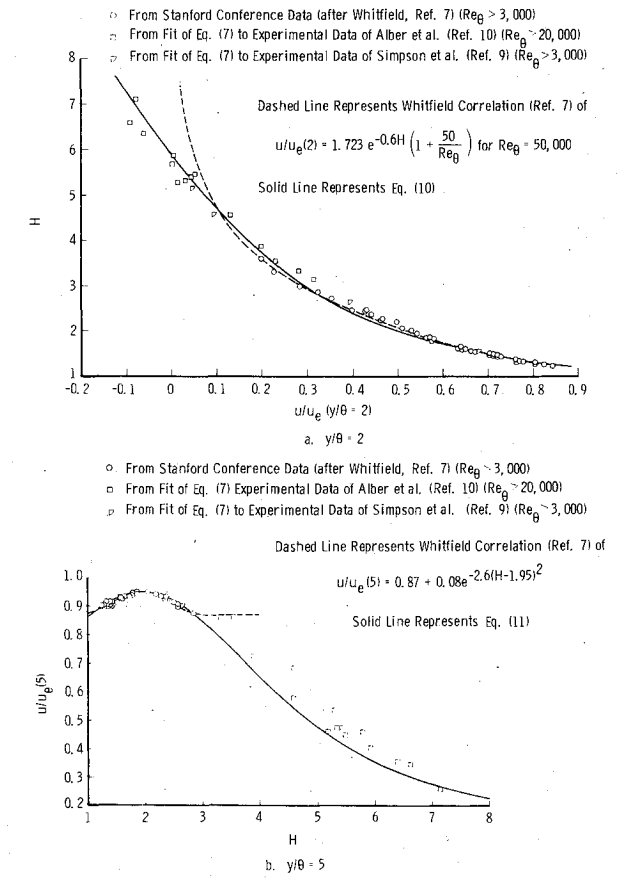

Fig. 3 Correlation of experimental velocity profile data.

correlations of u/u_e at $y/\theta=2$,

$$\frac{u}{u_e}(2)=\frac{1}{1.95}\left[\tanh^{-1}\left(\frac{8.5-H}{7.5}\right)-0.364\right] \tag{10}$$

and at $y/\theta=5$,

$$\frac{u}{u_e}(5)=0.155+0.795\,\mathrm{sech}\left[0.51\left(H-1.95\right)\right] \tag{11}$$

represent the measured data reasonably well. Both expressions approximate the Whitfield correlations[7] for $H<3$.

Thus, Eqs. (9-11) and (7) can be used to generate attached or separated, incompressible, turbulent boundary-layer velocity profiles from given H and Re_θ. This procedure is outlined in Table 1. For extension to compressible flow, the reader should consult Ref. 11.

Conclusions

An analytical expression that reasonably describes the velocity distribution in a separated two-dimensional turbulent boundary layer has been developed. The expression is an extension of the form derived by Whitfield[7] for attached flows on smooth, impermeable, adiabatic walls. The analytical expression was fit to experimentally measured attached and separated velocity profiles to establish a local skin friction correlation in the form $c_f=c_f(H,Re_\theta)$, which allows c_f to become negative, thus enabling attached or separated velocity profiles to be generated as a function of shape factor and momentum thickness Reynolds number. Because of the relatively small amount of experimental data which were available, the relations developed cannot yet be considered universally applicable to all flow situations. The correlations should be improved as more experimental data become available.

Acknowledgments

The author wishes to acknowledge Dr. David L. Whitfield, Professor of Aerospace Engineering, Mississippi State University, Mississippi State, Miss., who provided the foundation for this work. The research reported herein was conducted by the Arnold Engineering Development Center (AEDC), Air Force Systems Command. Work and analysis were done by personnel of Sverdrup Technology, Inc., AEDC Group, operating contractor for aeropropulsion testing at the AEDC.

References

[1] Kuhn, G. D. and Nielsen, J. N., "Prediction of Turbulent Separated Boundary Layers in Subsonic and Transonic Flow," AIAA Paper 73-663, July 1973.

[2] Cebeci, T., "Separated Flows and Their Representation by Boundary-Layer Equations," ONR-CR215-234-2, Sept. 1976.

[3] Moses, H. L., Jones, R. R. III, O'Brien, W. F., and Peterson, R. S. Jr., "Simultaneous Solution of the Boundary Layer and Freestream with Separated Flow," *AIAA Journal,* Vol. 16, Jan. 1978, pp. 61-66.

[4] Carter, J. E., "A New Boundary-Layer Interaction Technique for Separated Flow," AIAA Paper 79-1450, July 1979.

[5] Pletcher, R. H., "Prediction of Incompressible Turbulent Separating Flow," *Journal of Fluids Engineering,* Vol. 100, Dec. 1978, pp. 427-433.

[6] Whitfield, D. L., Swafford, T. W., and Jacocks, J. L., "Calculation of Turbulent Boundary Layers with Separation and Viscous-Inviscid Interaction," *AIAA Journal,* Vol. 19, Oct. 1981, pp. 1315-1322.

[7] Whitfield, D. L., "Analytical Description of the Complete Two-Dimensional Turbulent Boundary-Layer Velocity Profile," Arnold Air Force Station, Tenn., AEDC-TR-77-79 (ADA045033), Sept. 1977; see also, AIAA Paper 78-1158, July 1978.

[8] Whitfield, D. L., "Analytical, Numerical, and Experimental Results on Turbulent Boundary Layers," Arnold Air Force Station, Tenn., AEDC-TR-76-62 (ADA027588), July 1976.

[9] Simpson, R. L., Strickland, J. H., and Barr, P. W., "Features of a Separating Turbulent Boundary Layer in the Vicinity of Separation," *Journal of Fluid Mechanics,* Vol. 79, Part 3, March 1977, pp. 553-594.

[10] Alber, I. E., Bacon, J. W., Masson, B. S., and Collins, D. J., "An Experimental Investigation of Turbulent Transonic Viscous-Inviscid Interactions," *AIAA Journal,* Vol. 11, May 1973, pp. 620-627.

[11] Swafford, T. W., "Analytical Approximation of Two-Dimensional Separated Turbulent Boundary-Layer Velocity Profiles," Arnold Air Force Station, Tenn., AEDC-TR-79-99, Oct. 1980.

[12] Coles, D. E. and Hirst, E. A., eds., *Proceedings, Computation of Turbulent Boundary-Layers—1968 AFOSR-IFP-Stanford Conference: Vol. II, Compiled Data,* Thermosciences Div., Dept. of Mechanical Engineering, Stanford Univ., Calif., 1968.

[13] Ludweig, H. and Tillmann, W., "Untersuchugen uber die Wandschab-Spannung in turbulenten reibungschichten," *Ingeneur-Archiv,* Vol. 17, pp. 288-299; see also, NACA TM 1285, 1959.

[14] White, F. M., *Viscous Fluid Flow,* McGraw-Hill Book Company, New York, 1974.

Compressibility Effects in Turbulent Shear Layers

D. W. Bogdanoff*
University of Washington, Seattle, Washington

I. Introduction

FOR many reasons, it would be desirable to be able to make better predictions and to have a better understanding of the behavior of compressible turbulent shear layers. Such shear layers are important in the production of jet and rocket engine noise and are present in supersonic combustion jet engine designs. Compressible shear layers are also important in many high power laser systems.[1-3] The two-dimensional turbulent shear layer is well known to be strongly affected by compressibility.[4] In Sec. II of this Note, a Mach number M^+ is suggested which may be of value in correlating compressibility effects. In Sec. III, experimental results showing the decrease of shear layer width with increasing Mach number are compared with the corresponding variations of theoretical instability growth rates calculated by Blumen, et al.[5] In the final section, the significance of this comparison is discussed.

II. The Mach Number M^+

We denote velocity by u, density by ρ, specific heat ratio by γ, Mach number by M, and speed of sound by a. Subscripts *1* and *2* will refer to gases or conditions in the freestreams on the high- and low-speed sides of the shear layer, respectively. We define $\lambda_u = u_2/u_1, \lambda_\rho = \rho_2/\rho_1$, $\lambda_\gamma = \gamma_2/\gamma_1$, and $M_1 = u_1/a_1$. It seems reasonable to take the characteristic velocity to be $u_1 - u_2$. Since, in general, $a_1 \neq a_2$, there is a question as to the appropriate sound speed to be chosen. Two obvious candidates are the geometric and arithmetic average sound speeds. Instead of simply using one of these averages, we obtain M^+ from the following brief analysis.

It is assumed that there are certain large structures in the shear layer (this is known[6] to be the case for low-speed shear layers), and that these structures present similar profiles to the high- and low-speed streams and travel at a mean speed u_w. We estimate u_w by assuming that the total drag force on the large structures is zero, and therefore equate the dynamic pressure of the two freestreams with respect to the large structures, i.e.,

$$\left[1+\frac{\gamma_1-1}{2}\left(\frac{u_1-u_w}{a_1}\right)^2\right]^{\gamma_1/(\gamma_1-1)}-1 = \left[1+\frac{\gamma_2-1}{2}\left(\frac{u_w-u_2}{a_2}\right)^2\right]^{\gamma_2/(\gamma_2-1)}-1 \tag{1}$$

In support of Eq. (1), we note that in Brown and Roshko,[6] for $\lambda_u = 0.38$, $\lambda_\rho = 7$, and $M_1 \approx 0$, the mean observed speed of the large structures was $0.53u_1$. Using Eq. (1), $u_w = 0.55u_1$ is predicted. It is awkward, however, to obtain u_w from Eq. (1). Unless the Mach numbers are quite high and γ_1 and γ_2 are substantially different, Eq. (1) can be well approximated by

$$\rho_1(u_1-u_w)^2 = \rho_2(u_w-u_2)^2 \tag{2}$$

Using Eq. (2) to obtain u_w, we can easily obtain the Mach numbers of the large structures with respect to the two freestreams. We find

$$(u_1-u_w)/a_1 = M_1(1-\lambda_u)/(1+\lambda_\rho^{-1/2})$$

and

$$(u_w-u_2)/a_2 = M_1(1-\lambda_u)/[(1+\lambda_\rho^{-1/2})\lambda_\gamma^{1/2}]$$

We take M^+ to be the geometric average of these two Mach numbers, i.e.,

$$M^+ = \frac{M_1(1-\lambda_u)}{(1+\lambda_\rho^{-1/2})\lambda_\gamma^{1/4}} \tag{3}$$

Since λ_γ cannot normally be greater than 1.67 or less than 0.6, the difference between the geometric and arithmetic average values is very small.

III. Variation of Shear Layer Growth Rates with M^+, Theory and Experiment

Using M^+ as the correlation parameter, we compare the decrease in shear layer thickness with increasing Mach number observed experimentally with the corresponding decrease in the maximum linear instability growth rates from the theory of Blumen et al.[5] for a compressible, inviscid, constant density shear layer with a hyperbolic tangent velocity profile. The experimental data shown in Fig. 1 are taken from Brown and Roshko,[6] Maydew and Reed,[7] Ikawa and Kubota,[8] and Sirieix and Solignac[9] with the addition of the point at $M_1 = 5$ from Fig. 6 of Birch and Eggers.[4] The or-

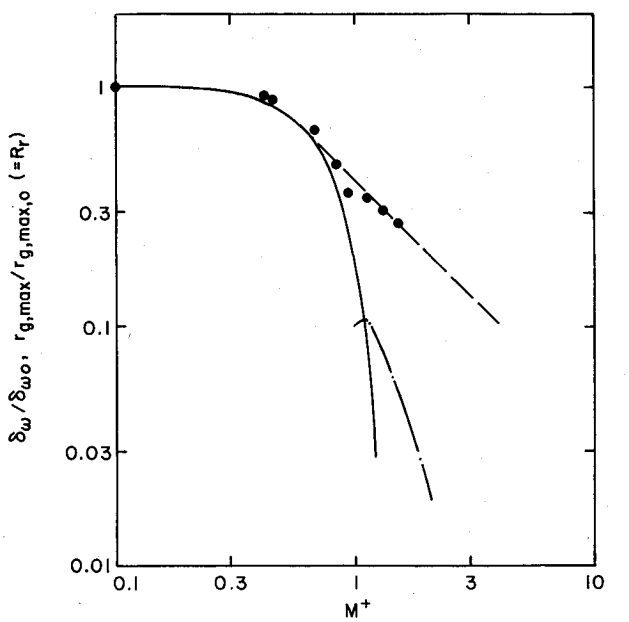

Fig. 1 Comparison of experimental and theoretical variations of shear layer growth rates with M^+. •, experimental values of δ_ω, normalized to unity at $M^+ = 0$. Curves are maximum inviscid instability growth rates ($r_{g,max}$) calculated by Blumen et al.[5] for several types of instabilities, also normalized to unity at $M^+ = 0$.

Received June 24, 1982; revision received Nov. 8, 1982.

*Research Engineer, Aerospace and Energetics Research Program. Member AIAA.